
Universiteit
Leiden
The Netherlands

High yield of B-branch electron transfer in a quadruple reaction center mutant of the photosynthetic bacterium Rhodobacter sphaeroides

Boer, A.L. de; Neerken, S.; Wijn, R. de; Permentier, H.P.; Gast, P.; Vijgenboom, E.; Hoff, A.J.

Citation
Boer, A. L. de, Neerken, S., Wijn, R. de, Permentier, H. P., Gast, P., Vijgenboom, E., & Hoff, A. J. (2002). High yield of B-branch electron transfer in a quadruple reaction center mutant of the photosynthetic bacterium Rhodobacter sphaeroides. *Biochemistry, 41*(9), 3081-3088. doi:10.1021/bi011450m

Version:	Publisher's Version
License:	Licensed under Article 25fa Copyright Act/Law (Amendment Taverne)
Downloaded from:	https://hdl.handle.net/1887/3239465

Note: To cite this publication please use the final published version (if applicable).

High Yield of B-Branch Electron Transfer in a Quadruple Reaction Center Mutant of the Photosynthetic Bacterium *Rhodobacter sphaeroides*†

Arjo L. de Boer,‡ Sieglinde Neerken,‡ Rik de Wijn,‡ Hjalmar P. Permentier,‡ Peter Gast,‡ Erik Vijgenboom,§ and Arnold J. Hoff*,‡

Department of Biophysics, Huygens Laboratory, and Leiden Institute of Chemistry, Gorlaeus Laboratories, Leiden University, Post Office Box 9504, 2300 RA Leiden, The Netherlands

Received July 12, 2001; Revised Manuscript Received November 20, 2001

ABSTRACT: A new reaction center (RC) quadruple mutant, called LDHW, of *Rhodobacter sphaeroides* is described. This mutant was constructed to obtain a high yield of B-branch electron transfer and to study $P^+Q_B^-$ formation via the B-branch. The A-branch of the mutant RC contains two monomer bacteriochlorophylls, B_A and β, as a result of the H mutation L(M214)H. The latter bacteriochlorophyll replaces bacteriopheophytin H_A of wild-type RCs. As a result of the W mutation A(M260)W, the A-branch does not contain the ubiquinone Q_A; this facilitates the study of $P^+Q_B^-$ formation. Furthermore, the D mutation G(M203)D introduces an aspartic acid residue near B_A. Together these mutations impede electron transfer through the A-branch. The B-branch contains two bacteriopheophytins, Φ_B and H_B, and a ubiquinone, Q_B. Φ_B replaces the monomer bacteriochlorophyll B_B as a result of the L mutation H(M182)L. In the LDHW mutant we find 35−45% B-branch electron transfer, the highest yield reported so far. Transient absorption spectroscopy at 10 K, where the absorption bands due to the Q_X transitions of Φ_B and H_B are well resolved, shows simultaneous bleachings of both absorption bands. Although photoreduction of the bacteriopheophytins occurs with a high yield, no significant (∼1%) $P^+Q_B^-$ formation was found.

Downloaded via LEIDEN UNIV on September 1, 2021 at 14:46:28 (UTC).
See https://pubs.acs.org/sharingguidelines for options on how to legitimately share published articles.

Despite the fact that the reaction center (RC)[1] of purple photosynthetic bacteria has two symmetrically arranged branches of cofactors, labeled A and B, that in principle could be used in charge separation, only one of them, branch A, is actually used. This is a conserved feature of RCs of purple bacteria and has also been found for the RC of the green filamentous bacterium *Chloroflexus aurantiacus*. Evidence for the preferential use of only one of the two branches comes primarily from studies on the bleaching of the absorption bands of the bacteriopheophytins H_A and H_B at cryogenic temperatures. At room temperature these bands overlap, but at cryogenic temperatures both the Q_X and the Q_Y absorption bands of the bacteriopheophytins become (more) resolved. Linear dichroism studies on single crystals from *Rhodopseudomonas viridis* RCs (*1*) and mutagenesis studies on RCs from *Rhodobacter capsulatus* (*2*) and *Rhodobacter sphaeroides* (*3*) have shown that the bacteriopheophytin used in charge separation is H_A. Both the Q_X and the Q_Y bands of H_A are red-shifted relative to the corresponding bands of H_B for RCs of *Rb. sphaeroides*, *Rb. capsulatus*, *Rps. viridis*, and *Cf. aurantiacus* (*4*−*6*). Bylina et al. (*2*) showed for *Rb. capsulatus* RCs that the red shift of H_A with respect to H_B is largely due to a glutamic acid residue in the L-subunit (L104 in *Rb. sphaeroides*), which forms a hydrogen bond to H_A. This residue is conserved in all purple bacterial RCs studied so far and in *Cf. aurantiacus*. In *Rps. viridis* RCs, H_A and H_B can be readily distinguished by their Q_Y absorption bands at 810 and 790 nm, respectively (*5*, *6*). After excitation of the primary electron donor P and subsequent electron transfer, a bleaching of the band at 810 nm but not of the band at 790 nm is observed, due to photoreduction of H_A but not of H_B. For RCs of *Rb. sphaeroides*, *Rb. capsulatus*, and *Cf. aurantiacus* the Q_X region is used to distinguish between H_A and H_B, due to the better resolution of the absorption bands in this region. For these RCs a bleaching of the H_A absorption band near 547 nm [*Rb. sphaeroides* and *Rb. capsulatus* (*7*)] or 540 nm [*Cf. aurantiacus* (*8*)] is observed but not of the H_B absorption band near 530 nm.

The branching ratio of A- vs B-side electron transfer is not known exactly, but the upper limit for the yield of $P^+H_B^-$ is a few percent. A direct estimate of the branching ratio by comparing the extent of bleaching of the H_A and H_B absorption bands at room temperature is not possible because these absorption bands overlap. At cryogenic temperatures, where these bands are resolved, an upper limit of ∼5% for electron transfer to H_B has been determined (*7*−*10*). An estimate for the extent of H_B bleaching near room temperature has been obtained by Heller et al. (*11*). They estimated electron transfer from P* to H_B to occur with a time constant, k_B, of 100 ps in a *Rb. capsulatus* RC mutant with impaired

† H.P.P. and R.d.W. acknowledge support from the Chemistry Division of The Netherlands Organization for Scientific Research (NWO).

* Author to whom correspondence should be addressed: phone +31-71-5275955; fax +31-71-5275819; e-mail hoff@biophys.LeidenUniv.nl.

‡ Department of Biophysics, Huygens Laboratory.

§ Leiden Institute of Chemistry, Gorlaeus Laboratories.

[1] Abbreviations: A-branch, active electron transport branch; B-branch, inactive electron transport branch; β-mutant, L(M214)H; DHW mutant, G(M203)D/L(M214)H/A(M260)W; $H_{A,B}$, pheophytin primary electron acceptors; LDHW mutant, H(M182)L/G(M203)D/L(M214)H/A(M260)W; P, primary electron donor; $Q_{A,B}$, quinone secondary electron acceptors; RC, reaction center.

10.1021/bi011450m CCC: $22.00 © 2002 American Chemical Society
Published on Web 02/05/2002

A-branch photochemistry. Since photoreduction of H_A in wild-type RCs occurs with a time constant of 3 ps, a branching ratio k_A/k_B of ~30 results for wild-type RCs, implying a yield of 3% for $P^+H_B^-$ (*11*). Another method of determining the ratio of A- vs B-side electron transfer was used by Kellogg et al. (*6*). They studied the formation of $P^+H_B^-$ in RCs that lacked Q_B and in which Q_A and H_A were already reduced. From the measured yield of $P^+H_B^-$ and the lifetime of P* in RCs with reduced Q_A and H_A [20 ps (*12*)], the branching ratio k_A/k_B was determined to be ~200.

It should be noted that assignment of the small absorbance changes that have been observed near 530 nm to photobleaching of H_B is not unambiguous. For instance, charge separation along the A-branch may induce an electrochromic shift of the H_B Q_X band or of the carotenoid absorption bands in the region of H_B Q_X absorption (in the case of carotenoid containing RCs) (*8, 11*). For *Cf. aurantiacus* RCs (with H_B absorbing at 530 nm and H_A at 540 nm) it has been shown that the bleaching observed near 530 nm, which is more pronounced than in *Rb. sphaeroides* RCs, is (largely) correlated with electron transfer through the A-branch (*8*). Absorption at 530 nm of multiple photons at high light intensity can cause B-side electron transfer, at least in *Rb. sphaeroides* (*13*).

Although photoreduction of H_B is usually not observed after a single excitation of P, Robert et al. (*4*) have shown that H_B^- can be accumulated by illumination of RCs poised at low redox potentials in the presence of the redox mediator methyl viologen. The mechanism of this reaction is not clear, but the fact that H_B^- can be photoaccumulated suggests $P^+H_B^-$ is formed in low yields in a single flash and that its formation is not thermodynamically impossible.

The origin of the preferential use of the A-branch in charge separation is not known. It can be argued that not understanding why the B-branch is not used is tantamount to not understanding A-branch electron transfer. Many studies have been aimed at getting insight in unidirectionality in terms of current electron transfer theories, and many attempts have been made to promote electron transfer through the B-branch (reviewed in ref 7; see also refs 11 and 14−18). Ideally one would like to have a detailed set of data on both electron transfer through the A-branch and electron transfer through the B-branch in order to evaluate the different physical factors that govern the direction of electron transfer in the RC. Most work has been done by use of site-directed mutagenesis for changing purported key amino acids in either the A- or B-chain. In some other work pigment modification has been employed. Success has been limited so far to ~35% B-chain transport (*17*). This situation has prompted us to further explore site-directed mutagenesis as a method to come to more strongly reduced A/B-branching ratios for electron transport in RCs of a purple bacterium.

In a previous article (*16*), we have described an RC triple mutant (labeled DHW) of *Rb. sphaeroides* with three mutations affecting charge separation through the A-branch. Two of these mutations, G(M203)D and L(M214)H, slow electron transfer through the A-branch. Due to the third mutation, A(M260)W, Q_A is absent, leaving Q_B as the only ubiquinone in the RC. Together, these mutations enable the study of Q_B photoreduction via the B-branch, which is the same as in wild-type RCs. Although the lifetime of P* in the DHW mutant was considerably longer than the P* lifetime in wild-type RCs, bleaching of the absorption band of H_B could not be demonstrated (upper limit less than 5% of the bleaching of H_A in wild-type RCs). The state $P^+Q_B^-$ was formed with a low yield (<5%) and could not be photoaccumulated.

Recently, RCs of *Rb. sphaeroides* were described in which the monomer bacteriochlorophyll B_B was replaced by a bacteriopheophytin, Φ_B, due to the mutation H(M182)L (*17*). In the following, these RCs will be called Φ_B RCs. In Φ_B RCs B-branch electron transfer with a yield of ~35% was reported, resulting in the formation of $P^+\Phi_B^-$ (*17*). Also recently, Kirmaier et al. (*15*) showed that when mutations impeding A-branch electron transfer in the RC of *Rb. capsulatus* were combined with a mutation that presumably raises the B_B^-/B_B midpoint potential, these mutations cooperated to result in $P^+H_B^-$ formation with a yield of 25%. By analogy, replacement of B_B with Φ_B in the *Rb. sphaeroides* RCs combined with mutations that (partially) impede A-branch electron transfer should lead to increased B-branch electron transfer. The quadruple mutant described in the present article was designed with this objective. It was constructed by introducing the mutation H(M182)L, resulting in the replacement of B_B with Φ_B, in the DHW mutant that was described previously (*16*). In summary, the resulting quadruple mutant, LDHW, has the following mutations (see Figure 1): (1) H(M182)L, which results in the incorporation of a bacteriopheophytin molecule, Φ_B, for B_B; (2) G(M203)D, making the transfer of an electron from P* to B_A more difficult; (3) L(M214)H, which results in the incorporation of a bacteriochlorophyll molecule, β, instead of the bacteriopheophytin molecule H_A; (4) A(M260)W, leading to the rigorous exclusion of Q_A from the reaction center (*19, 20*). The mutations G(M203)D and L(M214)H cooperate to slow electron transfer through the A-branch (*16*). The high yield of "wrong way" electron-transfer expected for the LDHW mutant and the presence of Q_B as the sole quinone molecule would make this mutant a suitable system for studying photoreduction of Q_B via the B-branch.

We find that (i) P* decay is faster in LDHW RCs than in DHW RCs [which do not contain the H(M182)L mutation; see ref 16)]; (ii) the yield of B-branch electron transfer in LDHW RCs at room temperature is 35−45%; (iii) the Q_X absorption bands of both bacteriopheophytins of the B-branch are simultaneously (partially) bleached; (iv) the ratio of the magnitude of these bleachings remains constant with time; and (v) no significant (~1%) formation of $P^+Q_B^-$ occurs, suggesting that electron transfer from H_B^- to Q_B is not efficient enough to compete with charge recombination processes.

MATERIALS AND METHODS

Bacterial Strains, Growth, Mutagenesis, and Isolation of the Reaction Center. We have used the mutagenesis system originally developed by Paddock et al. (*21*), with some minor modifications (*16*), to introduce mutations in the M subunit of the RC of *Rb. sphaeroides*. Site-directed mutations in the *pufM* gene were made by the following codon changes: CAC → CTG (M182 H → L), GGT → GAC (M203 G → D), CTG → CAC (M214 L → H), and GCC → TGG (M260 A → W). Cell growth and the procedure of isolating wild-type and mutant RCs were as described in ref 16.

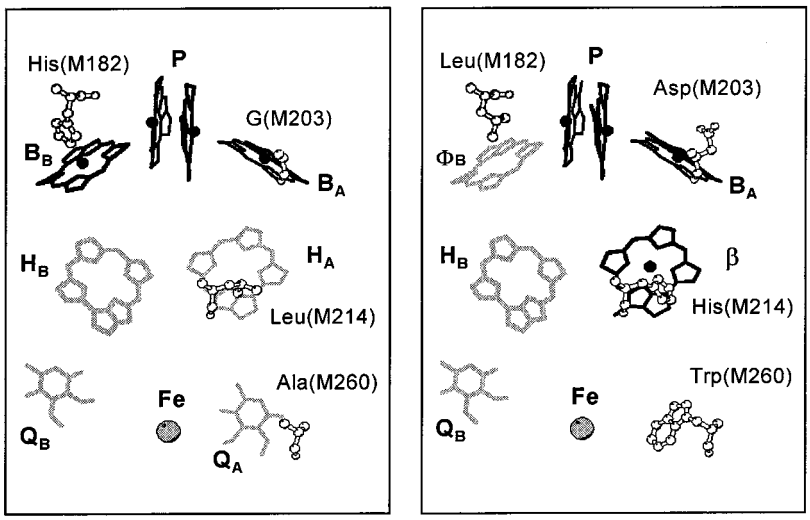

FIGURE 1: Schematic representation of the cofactors in wild-type RCs (left panel) and LDHW RCs (right panel). Amino acid residues that have been mutated are also shown. For clarity only the porphyrin rings of the bacteriochlorophylls and bacteriopheophytins are shown, and the carotenoid and isoprenoid tails of the quinones have been omitted. See text for details. After Ermler et al. (*32*), drawn with the Molscript program (*33*).

Steady-State Spectroscopy. Steady-state absorption spectroscopy was performed on a single-beam spectrophotometer (*22*). Glycerol was added to all samples used in low-temperature experiments to a final concentration of 67% (v/v).

EPR Measurements. The electron paramagnetic resonance measurements were performed at 20 K with a home-built phase-sensitive homodyne combined pulsed and continuous wave (cw) EPR spectrophotometer.

Charge Recombination and Yield of $P^+Q_B^-$. Formation and recombination of $P^+Q_B^-$ at room temperature were studied by monitoring the bleaching of the P band near 865 nm following subsaturating filtered flash light provided by a xenon flash lamp. A home-built single-beam spectrophotometer (*23, 24*) was used to generate and record the kinetic data. The same apparatus was used to determine the yield of $P^+Q_B^-$ formation. Here, subsaturating light from a tungsten halogen lamp filtered by an 860 nm interference filter was used to excite the Q_Y band of P at 865 nm. The amplitude of the resulting bleaching of the Q_X band of P near 600 nm was measured as a function of the illumination time for samples of wild-type and mutant RCs with identical absorptions at 865 nm. A 10-fold excess of UQ_{10} was added to the RCs to ensure full occupation of the Q_B site. The quantum yield for $P^+Q_B^-$ formation in DHW RCs was determined by comparing the initial slopes obtained for wild-type and mutant RCs and with the assumption of a 100% quantum yield for $P^+Q_B^-$ formation in wild-type RCs.

Picosecond Transient Absorption Spectroscopy. Time-resolved transient absorption difference measurements at room temperature were performed with a home-built amplified dye laser system with continuum generation and optical multichannel analyzer (OMA) detection, operating at 10 Hz, described by Kennis et al. (*25, 26*). The time resolution was 600 fs. Excitation pulses were obtained by amplification of the continuum in a dye cell (LDS 867, Exciton). Wavelengths shorter than 850 nm were cut off with an RG850 filter (Melles Griot, Irvine, CA). Pump and probe pulses were polarized parallel to each other for better signal-to-noise. The influence of nonisotropic excitation of P and parallel probing of H_A^- in WT RCs and H_B^- and Φ_B^- in the LDHW mutant can be calculated with the formalism of photoselection. With the assumption that the Q_y transitions are along the N_1-N_3 axes as given by the crystal structure and assuming identical molar extinction coefficients (see below), we find correction ratios $A_{II}(\Phi_B)/A_{II}(H_A) = 2.66$ and $A_{II}(H_B)/A_{II}(H_A) = 1.11$, respectively, compared to ratios of unity for magic angle probing.

The samples contained 0.5 mM terbutryn to inhibit $P^+Q_B^-$ formation and were kept in a moving cuvette (optical pathway 1 mm) in order to avoid accumulation of photooxidized P. The absorbance was adjusted to 1.0/mm at the wavelength of interest. Excitation was in the primary donor band. Approximately 5−10% of the P absorption band was bleached per laser pulse.

RESULTS AND DISCUSSION

The combination of mutations G(M203)D and L(M214)H that inhibit A-branch electron transfer with the H(M182)L mutation that promotes B-branch electron transfer (*17*) was expected to result in a high yield of B-branch electron transfer, eventually leading to the formation of $P^+Q_B^-$ exclusively via the B-branch.

Absorption Spectra. Absorption spectra at 6 K of wild-type, DHW, and LDHW RCs are shown in Figure 2. The absorption spectra are different from each other because of the mutations that affect the cofactor composition of the RC. The absorption spectrum of the DHW mutant, which was described in detail in ref 16, differs from the wild type due to the replacement of the bacteriopheophytin H_A with the β bacteriochlorophyll molecule (Figure 1). In the absorption spectrum, this replacement is reflected by the disappearance of the Q_X band due to H_A at 547 nm, by the decreased amplitude of the band near 760 nm (which in wild-type RCs is due to the Q_Y transitions of both H_A and H_B but in the DHW mutant is due to the Q_Y transition of H_B only), and by the appearance of a new band at 784 nm due to the Q_Y transition of β. The H(M182)L mutation of the LDHW mutant results in the replacement of B_B with the Φ_B bacteriopheophytin (*17*). As a consequence of this replace-

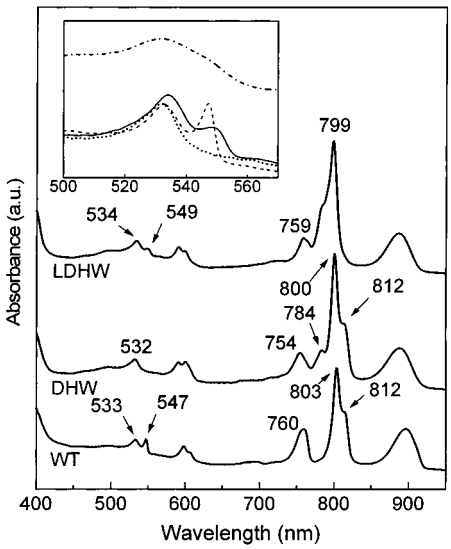

FIGURE 2: Low temperature (6 K) absorption spectra of wild-type (WT), DHW, and LDHW RCs. The inset shows the bacteriopheophytin Q_X absorption bands of WT RCs (---), DHW RCs (▪▪▪), and LDHW RCs (—). The spectra were normalized to the same absorbance at the maximum of the P band. The upper curve (— • —) in the inset represents the Q_X absorption bands in LDHW RCs at room temperature.

ment, the absorption band at 812 nm due to the Q_Y transition of B_B, which is visible as a shoulder of the Q_Y absorption band of B_A near 800 nm in the spectra of wild-type and DHW RCs, is absent in the absorption spectrum of the LDHW mutant. Instead, a shoulder has now appeared at the blue side of the band near 800 nm. We ascribe this shoulder to the Q_Y absorption of both Φ_B and β. As is described in ref 16, the location of the Q_Y absorption band of β is quite variable. In the absorption spectrum of the L(M214)H single mutant the absorption maximum is at 779 nm, while it is at 775 and 784 nm in the absorption spectra of two other mutants studied in ref 16, the G(M203)D/L(M214)H (DH) and the G(M203)D/L(M214)H/A(M260)W (DHW) mutants, respectively. Considering this range of positions for the absorption maximum of β, it is likely that β mostly contributes to the blue side of the shoulder and that Φ_B contributes more to the red side of the shoulder. Replacement of B_B with Φ_B also introduces a new band at 549 nm. This band is due to the Q_X transition of Φ_B. Its position is different from that of the Q_X absorption of H_B at 534 nm and resembles the position of the H_A Q_X band at 547 nm in wild-type RCs. Although the positions of the Q_X absorption bands of Φ_B and H_A are similar, their shapes are quite different (Figure 2, inset). The absorption band of Φ_B is much broader than that of H_A (more like H_B), and the amplitude is lower. LDHW RCs have two bacteriopheophytins in the B-branch and none in the A-branch. The molar extinction coefficients of H_B and Φ_B are largely the same as judged from the low-temperature absorption spectra. B-branch electron transfer in LDHW RCs can be monitored by studying bleaching of the absorption bands due to the bacteriopheophytins. Furthermore, since the absorption maxima of the two bacteriopheophytins have different positions, it is possible to observe photoreduction of each of them separately.

Picosecond Transient Absorption Spectroscopy at Room Temperature. Picosecond transient absorption measurements were performed in the presence of terbutryn to prevent the photoaccumulation of the long-lived $P^+Q_B^-$ state with the laser system operating at 10 Hz. Absorption difference spectra obtained for the LDHW mutant in the absorption band of P near 865 nm at several delay times are shown in Figure 3. Absorption changes in this region are due to bleaching of the 865 nm band on which stimulated emission of P* between 870 and 1000 nm is superimposed. As in wild-type RCs, the stimulated emission in LDHW RCs decays as P* disappears by charge separation. In wild-type RCs, charge separation in the presence of terbutryn leads to the formation of the state $P^+Q_A^-$. This state does not appreciably decay on the picosecond or nanosecond time scale. Thus, no P recovery is visible on these time scales and the bleaching near 865 nm persists. In contrast, in LDHW RCs charge separation does not lead to the formation of such relatively long-lived states, since these RCs contain neither Q_A [due to the A(M260)W mutation] nor Q_B (due to the presence of terbutryn). Instead, relatively short-lived states are formed that recombine on the picosecond to nanosecond time scale and lead to recovery of P and hence to a decay of the bleaching near 865 nm. In Figure 4 the P* decay kinetics and fits for both DHW and LDHW RCs are shown. The fast component of P* decay in LDHW RCs is about twice as large as that in DHW RCs. This is in keeping with the assumption that B-branch electron transfer is possible as an

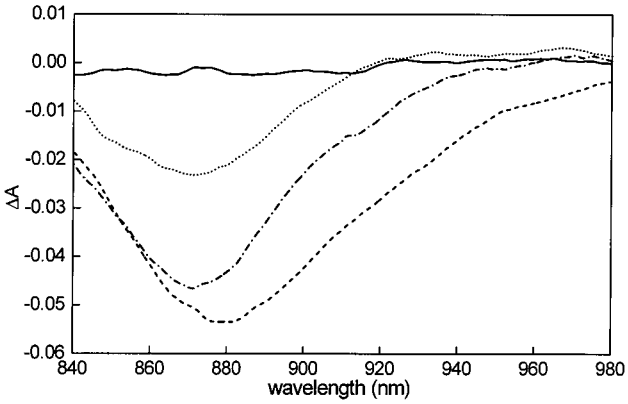

FIGURE 3: Transient absorption difference spectra at room temperature at the long-wavelength absorption band of P for LDHW RCs. Shown are spectra before excitation (—) and at delay times of 1 ps (---), 8 ps (— • —), and 450 ps (▪▪▪).

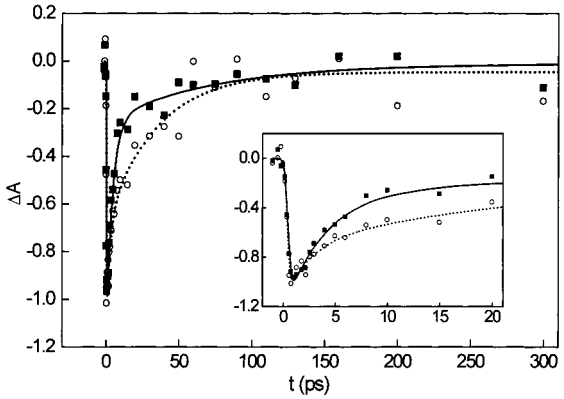

FIGURE 4: Kinetics of P* decay at room temperature, averaged between 920 and 930 nm. (○, ▪▪▪) Transient absorption data and a biexponential fit obtained for DHW RCs; (■, —) data and a biexponential fit obtained for the LDHW mutant. The data were normalized to have identical initial bleachings of P. The inset shows the data between 0 and 20 ps.

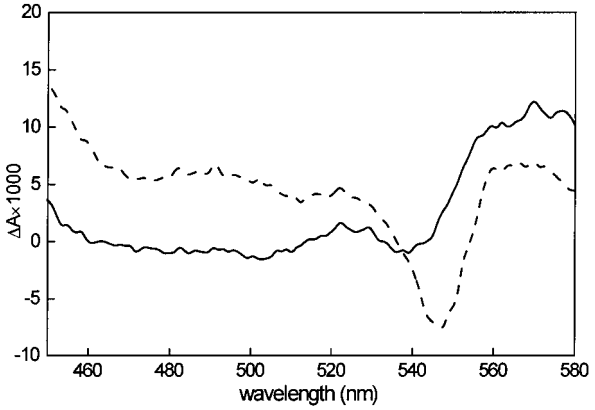

FIGURE 5: Absorption difference spectra at room temperature of wild-type and LDHW RCs in the Q_X region where the bacteriopheophytins absorb. The bleaching at 545 nm in the spectrum for wild-type RCs after a delay time of 10 ps (---) is due to photoreduction of H_A. The bleaching at 540 nm in LDHW RCs at a delay time of 30 ps (—) is due to photoreduction of Φ_B and H_B, the bacteriopheophytins in the B branch of this mutant (see text for details). The spectra were normalized to have identical initial bleachings of P.

extra, alternative channel for charge separation in LDHW RCs. For both RCs two exponential components are required to obtain an adequate fit. A biexponential fit yielded time constants of 2.5 ± 0.8 ps (40%) and 36 ± 5 ps (60%) for the DHW mutant, and for the LDHW mutant, time constants of 3.7 ± 0.8 ps (85%) and 63 ± 7 ps (15%). P* decay also has been reported to be faster in Φ_B RCs [RCs that only have the H(M182)L mutation] than in wild-type RCs (*17*). Single-exponential fits of their P* decays yielded time constants of 2.6 and 3.1 ps for Φ_B and wild-type RCs, respectively.

Evidence for B-branch electron transfer in LDHW RCs is presented in Figure 5, where absorption difference spectra in the Q_X region of the bacteriopheophytins are shown for wild-type and LDHW RCs. In the wild-type spectrum a strong bleaching at 545 nm (due to photoreduction of H_A) is superimposed on a broad, essentially featureless absorption band. This broad absorption band is always present, at short as well as at longer delay times (*3, 9, 27*), suggesting that it is associated with P* as well as P^+. A similar broad, featureless absorption band was observed for the DHW mutant at all delay times after P* formation (*16*). For unknown reasons, for the LDHW mutant there is no such absorption increase in the 460−520 nm region of the difference spectrum, nor is it visible in the data presented for Φ_B RCs (*17*). There is some absorption, however, between 525 and 570 nm. Superimposed on this absorption there is a trough near 540 nm. The position of the trough corresponds to the position of the bleaching at 538 nm that has been found in Φ_B RCs (*17*). This bleaching was ascribed to photoreduction of Φ_B and it was concluded that no further electron transfer to H_B occurs in Φ_B RCs. As will be shown below, low-temperature experiments with LDHW RCs provide evidence for simultaneous, partial bleaching of the absorption bands of both H_B and Φ_B. At room temperature, where the Q_X absorption bands of H_B and Φ_B are not resolved, only one negative band is visible, centered near 540 nm.

Picosecond Transient Absorption Spectroscopy at 10 K. Transient absorption difference spectra in the Q_Y region at

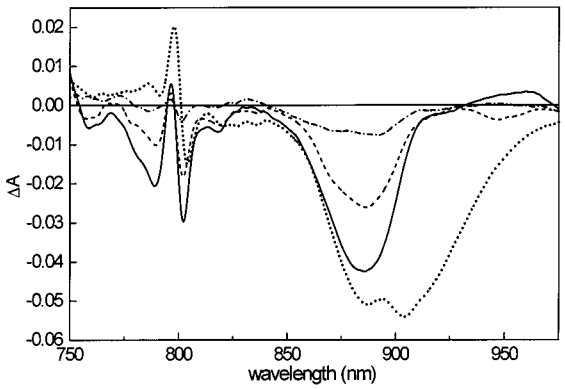

FIGURE 6: Absorption difference spectra in the Q_Y region for LDHW RCs at 10 K. The spectra were taken at delay times of 1 ps (▪▪▪), 30 ps (—), 450 ps (---), and 1.9 ns (— • —).

10 K obtained for the LDHW mutant at several delay times are shown in Figure 6. The spectrum at a delay time of 1 ps primarily represents the excited state of P. There is a large bleaching near 890 nm, where P absorbs. Superimposed on the red side of this bleaching is a band due to stimulated emission from P*. Signals around 800 nm are ascribed to changes in the excitonic interactions between P and B_A (*7*), since B_B has been replaced with Φ_B, which absorbs near 790 nm. The new feature near 790 nm may then reflect changes in the interaction between P and Φ_B. In the spectrum at 30 ps the stimulated emission has largely disappeared due to charge separation. A strong bleaching has developed near 790 nm, with a shoulder near 780 nm. As discussed in an earlier section, both Φ_B and β contribute to the shoulder on the blue side of the band of B_A near 800 nm, with β probably contributing more to the blue side of this shoulder. Accordingly, the strong bleaching near 790 nm in the absorption difference spectrum is likely due to bleaching of the Φ_B Q_Y band, while the shoulder near 780 nm is due to bleaching of the β Q_Y band. The absorption changes near 755 nm are related to H_B. Possible contributions in this region are a bandshift of the H_B Q_Y band due to photoreduction of Φ_B as well as bleaching of the H_B Q_Y band due to its own photoreduction.

The shape of the spectra at 450 ps and at 1.9 ns is largely the same as that of the 30 ps spectrum, although the amplitudes of the absorption and bleaching maxima have decreased because some recombination of charge-separated states has occurred. These data suggest that the charge-separated states in LDHW RCs, $P^+\Phi_B^-$, $P^+H_B^-$, and $P^+\beta^-$ (and possibly $P^+B_A^-$), decay with approximately the same time constants. This interpretation is consistent with the room-temperature data obtained for the DHW mutant, where the bleaching of P also has largely vanished after 1.9 ns (*16*). Recombination of $P^+\Phi_B^-$ in Φ_B RCs (at room temperature) was reported to occur with a time constant of 200 ps (*17*).

Absorption difference spectra in the Q_X region obtained at 10 K for the LDHW mutant are shown in Figure 7. Spectra taken at 25, 30, and 40 ps (—) and at 400, 500, and 700 ps (▪▪▪) were identical and have been averaged. As for the room-temperature spectra, there is some positive absorption between 525 and 570 nm. Superimposed on this absorption there are two troughs of about equal amplitude with minima at 534 and 549 nm that correspond to the positions of the Q_X bands of H_B and Φ_B, respectively, and presumably are

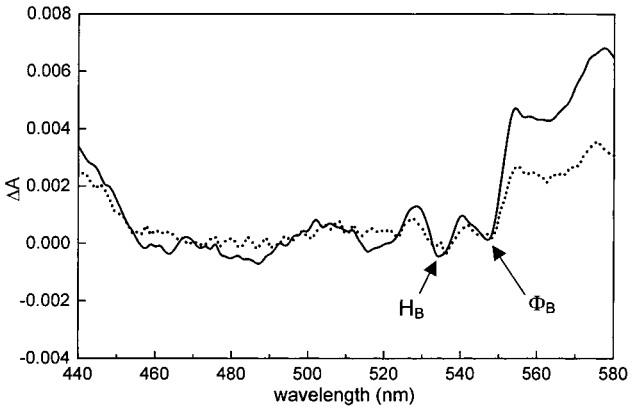

FIGURE 7: Absorption difference spectra at 10 K for LDHW RCs in the Q_X region of the bacteriopheophytins. (—) Average of spectra at delay times of 25, 30, and 40 ps; (•••) average of spectra at delay times of 400, 500, and 700 ps. Arrows indicate the positions of the bleachings of the bacteriopheophytins of the B branch in LDHW RCs.

due to (partial) bleaching of these bands. The shape of the difference spectra shown in Figure 7 at different delay times is essentially the same. Since the bleachings at 534 and 549 nm appear and disappear simultaneously, it is likely that they result from an equilibrium between the states $P^+\Phi_B^-$ and $P^+H_B^-$. The bleaching near 540 nm that has been observed at room temperature in the absorption difference spectra for Φ_B RCs and LDHW RCs probably represents overlapping bleachings due to the formation of $P^+\Phi_B^-$ and $P^+H_B^-$. Since the B-branch in our quadruple mutant is identical to that of the Φ_B mutant, the conclusion of Katilius et al. (*17*) that B-branch electron transfer in Φ_B RCs is limited to the formation of $P^+\Phi_B^-$ (that is, there is no further electron transfer to H_B) likely needs revision.

B-Chain Electron Transport. When the extent of B-chain electron transport is determined from the bleaching near 540 nm, it is important to assess whether it represents photoreduction of the two B-chain bacteriopheophytins in LDHW RCs or whether it is possibly (partly) due to bandshifts of H_B and/or Φ_B resulting from charged cofactors in the A- and/or B-chain. Since the shape of the broad new band between 520 and 570 nm is unknown, such assessment is not unambiguous. We have, however, a number of independent arguments that most of the absorption changes at 540 (room temperature) and 534 and 549 nm (10 K) are indeed due to bleachings.

First, charge separation in the H(M182)L mutant is faster than in WT RCs (*17*), and in the LDHW mutant, faster than in the DHW mutant. This indicates that there is an extra channel for charge separation competing with the A-chain.

Second, the 30 ps spectrum of Figure 6 shows between 770 and 820 nm, where β and Φ_B absorb, a strong absorbance decrease, not just one or more shifts. An absorbance change at 790 nm is also observed by Katilius et al. (*17*), whose mutant does not contain the β pigment. The β pigment shows a small absorbance at 784 nm (*15, 16*) and if bleached would contribute only little to the bleaching at 790 nm. Since the band at 549 nm is clearly related to Φ_B, its change concomitant with the bleaching of the 790 nm band strongly suggests that this change is also a bleaching.

Third, we and others (*15, 16*) have not observed a shift of H_B due to reduction of the $B_A\beta$ complex in the β-mutants. Since there is no H_A present in the LDHW mutant, a shift of H_B due to H_A^- as suggested in ref 8 for *Cf. aurantiacus* RCs cannot occur. This purported shift followed the kinetics of H_A^- and not of P^+. Neither were there indications for a P^+-induced shift of Φ_B in the nanosecond difference spectrum of Q_A-containing *Cf. aurantiacus* RCs.

Fourth, a remaining shift mechanism would be a shift of the Q_x band of Φ_B by H_B^- or that of H_B by Φ_B^-. In that case at least half of the unresolved absorbance changes in the Q_x band region observed at room temperature (Figure 5) would be due to a bleaching of either Φ_B or H_B or both. In view of the data in Figure 2 and Figure 6, we believe that in the difference spectrum of Figure 7 the feature at 549 nm represents a photoreduction. Then, the feature at 534 nm cannot be a band shift, because it lacks the derivative shape. This lack can no longer be explained by the assumption of two overlapping band shifts in opposite direction. We conclude that the two features are due to photoreduction. By inference, also the absorbance change at 540 nm in the spectrum of Figure 5 is then due to photoreduction of the two B-chain bacteriopheophytins.

For assessing the extent of B-chain activity, the broad new band in the 520−560 region was approximated by the tail of a broad Gaussian peaking at about 570 nm for LDHW RCs and by a straight line connecting the data at 520 and 570 nm for wild-type RCs (spectra taken under identical conditions and normalized at the initial P band bleaching due to P* formation). The amplitude of the two bands at 534 and 549 nm in the low-temperature spectrum of Figure 7 is about the same. By inference, the measured amplitude of the contribution of the bleaching of Φ_B and H_B is then also similar in the room-temperature spectrum of Figure 5. The ratio of the area between the baseline and the trough at 540 nm in the difference spectrum for LDHW RCs to the corresponding area at 545 nm for wild-type RCs (which corresponds to 100% A-chain electron transport) is an estimate for the relative bleaching of the bacteriopheophytin absorption bands in the A- and B-chain when the appropriate correction factors for parallel probing are taken into account (see Materials and Methods). We thus obtain a yield of B-branch electron transfer in LDHW RCs of 35−45%.

We note that Katilius et al. (*17*) could only estimate the yield of B-branch charge separation in Φ_B RCs in an indirect way by virtue of the fact that the charge-separated state(s) in this branch recombine(s) with a time constant of 200 ps, much faster than charge recombination of $P^+Q_A^-$ or $P^+H_A^-$ in the A-branch, which typically occur with time constants of 100 ms and ∼10 ns, respectively. In contrast, our determination of 35−40% for B-branch charge separation relies directly on the bleaching of the bacteriopheophytin(s) involved. Interestingly, a yield of ∼30% B-chain electron transport was obtained for the β-mutant of *Rb. capsulatus* in which additionally the Tyr(M208), corresponding to Tyr(M210) in *Rb. sphaeroides*, was swapped with the symmetry-related Phe(L181) (*28*). This result and ours suggest that the relative position of the energy levels of the ion pairs $P^+B_A^-$ and $P^+B_B^-$ with respect to P* is an important factor in determining the branching ratio.

$P^+Q_B^-$ Formation at Room Temperature. $P^+Q_B^-$ formation in LDHW RCs was studied by monitoring light-induced changes on the time scale of (milli)seconds at the absorption band of P at 865 nm at room temperature. Since Q_B is usually

largely lost during RC preparation, excess UQ_{10} (at least 10-fold) was added to the RCs to repopulate the Q_B site. Despite the high yield of 35−45% for B-branch electron transfer in the LDHW mutant, no significant (∼1%) formation of $P^+Q_B^-$ could be observed. This contrasts with our experimental data for the DHW mutant, where electron transfer from H_B to Q_B proceeds with ∼100% yield (*16*). One explanation would be that the Q_B site in LDHW RCs is not populated, even after addition of extra UQ_{10}. Thus either the H(M182)L mutation or the ensemble of mutations in LDHW RCs may prevent binding of UQ_{10} in the Q_B site. This is not very likely, however, since none of the mutations is located in the vicinity of the Q_B binding pocket. Also, recent detailed X-ray crystallographic analysis of the A(M260)W single mutant showed a high occupancy of the Q_B site (*29*). Another explanation is that electron transfer from H_B^- to Q_B cannot compete with recombination between $(\Phi_B,H_B)^-$ and P^+. Indeed, recombination between $(\Phi_B,H_B)^-$ and P^+ occurs with a time constant of ∼200 ps (*17*) and thus is much faster then what would be expected for recombination between H_B^- and P^+ (∼10 ns by anology with $P^+H_A^-$ recombination in the A-branch of wild-type RCs).

We may estimate the rate of electron transfer from $(\Phi_B,H_B)^-$ to Q_B in the LDHW mutant by considering the time constant of charge recombination of the ($P^+\Phi_B^-$, $P^+H_B^-$) states in the B-branch, about 200 ps (*17*), and the yields of the formation of these states and that of $P^+Q_B^-$. Since the mixture of the states $P^+\Phi_B^-$ and $P^+H_B^-$ is formed with a yield of 35−45% and since $P^+Q_B^-$ is formed with a yield of ∼1%, electron transfer from the states $P^+\Phi_B^-$ and $P^+H_B^-$ to Q_B must be ∼40 times slower than charge recombination of these states, implying a time constant of ∼10 ns for electron transfer to Q_B. Thus electron transfer to Q_B in the LDHW mutant is much slower than electron transfer from H_A to Q_A in the A-branch of wild-type RCs. One explanation may be that the Q_B binding pocket differs from that of Q_A. For instance, Stilz et al. (*30*) have observed that in *Rb. capsulatus* the mutation W(M250)F decreases the rate of electron transfer from H_A^- to Q_A by a factor of 4. This suggests that M250W, and its analogue M252W in *Rb. sphaeroides*, acts as a superexchange conduit for electron transfer in the A-chain. In the B-chain the symmetry-related residue of M252W is a phenylalanine. Another explanation is that, in LDHW RCs, electron transfer to Q_B is not purely from H_B^- but from $(\Phi_B,H_B)^-$. This leads to a larger (average) electron-transfer distance and a resulting slowing down of the electron transfer as described by nonadiabatic electron transfer theory.

Photoaccumulation of $P^+Q_B^-$ at 20 K. Although $P^+Q_B^-$ in LDHW RCs is formed with a low yield of ∼1%, presumably due to fast recombination of early intermediates in the charge separation sequence, prolonged illumination of these RCs should result in a appreciable population of the long-lived $P^+Q_B^-$ state. This state was found to decay with a time constant of several seconds in DHW RCs (*15*). We could not photoaccumulate the $P^+Q_B^-$ state under continuous illumination at 20 K, as evidenced by our inability to detect the EPR signal due to Q_B^-. Previously, we were also unable to detect photoaccumulation of $P^+Q_B^-$ in DHW RCs (*16*).

Interestingly, Q_B in the A(M260)W mutant is located in a proximal site relative to the non-heme iron, in contrast to Q_B in wild-type RCs, which is located in a distal position displaced by about 6 Å in the direction of H_B (*31*). Assuming that, unlike electron transfer from H_A^- to Q_A in its (proximal) site, H_B^- cannot transfer electrons to Q_B in the proximal position, this observation would explain our inability to photoaccumulate $P^+Q_B^-$ in both the LDHW and the DHW mutants. At room temperature Q_B may move freely between the distal and proximal sites, whereas it may be frozen preferentially at the proximal site at 20 K. These assumptions may explain why electron transfer from H_B^- to Q_B in DHW RCs occurs with a 100% yield at room temperature while no photoaccumulation occurs at 20 K. The same reasoning holds for LDHW RCs, with the extra argument that electron transfer to Q_B is by now much impaired as compared to DHW RCs (see above). As the distances between H_A and Q_A, and between H_B and Q_B in the proximal position, are about the same, the difference in transfer rate is likely due to a difference in reorganization energy.

We note that the B-branch of LDHW RCs has an analogue in an RC mutant of *Rps. viridis* (*32*). In this RC mutant, B_A is replaced by a bacteriopheophytin molecule, which we shall call Φ_A. Thus, this mutant has an A-branch that contains two bacteriopheophytins (Φ_A and H_A), whereas in Φ_B and LDHW RCs the B-branch contains two bacteriopheophytins. In *Rps. viridis* Φ_A RCs, charge separation results in a mixture of the states $P^+\Phi_A^-$ and $P^+H_A^-$. Subsequent $P^+Q_A^-$ formation occurs with a yield of 50%, whereas ground-state recovery of P accounts for the remaining 50%. Both decays occur with a time constant of 140 ps (*32*). Thus, the time constant for electron transfer from $P^+\Phi_A^-$ and $P^+H_A^-$ to Q_A is similar to the time constant for electron transfer from H_A to Q_A in wild-type RCs [200 ps (*7*)] and much smaller than the time constant of 10 ns for electron transfer from $P^+\Phi_B^-$ and $P^+H_B^-$ to Q_B in LDHW RCs.

CONCLUSIONS

By combining mutations that impede A-branch electron transfer with a mutation that facilitates electron transfer through the B-branch, an RC mutant was created in which 35−45% B-branch electron transfer occurs. This is the highest yield reported so far. The B-branch of the mutant contains two monomeric bacteriopheophytin molecules, Φ_B and H_B. Low-temperature transient absorption studies show that charge separation through the B-branch leads to an equilibrium between $P^+\Phi_B^-$ and $P^+H_B^-$. Further electron transfer to Q_B occurs with a very low yield (∼1%). We conclude that electron transfer from $P^+\Phi_B^-$ and $P^+H_B^-$ to Q_B cannot compete with charge recombination.

ACKNOWLEDGMENT

We are indebted to Dr. I. V. Borovykh for carrying out the EPR experiments and to A. H. M. de Wit for his help in growing the bacteria.

REFERENCES

1. Zinth, W., Sander, M., Dobler, J., Kaiser, W., and Michel, H. (1985) in *Antennas and reaction centers of photosynthetic bacteria* (Michel-Beyerle, M.-E., Ed.) pp 97−102, Springer-Verlag, Berlin and New York.
2. Bylina, E. J., Kirmaier, C., McDowell, L., Holten, D., and Youvan, D. C. (1988) *Nature 336*, 182−184.

3. Kirmaier, C., Gaul, D., DeBey, R., Holten, D., and Schenck, C. C. (1991) *Science 251*, 922−927.
4. Robert, B., Lutz, M., and Tiede, D. M. (1985) *FEBS Lett. 183*, 326−330.
5. Tiede, D. M. (1987) *Photochem. Photobiol. Suppl. 45*, 42−42.
6. Kellogg, E. C., Kolaczkowski, S., Wasielewski, M. R., and Tiede, D. M. (1989) *Photosynth. Res. 22*, 47−59.
7. Woodbury, N. W., and Allen, J. P. (1995) in *Anoxygenic photosynthetic bacteria* (Blankenship, R. E., Madigan, M. T., and Bauer, C. E., Eds.) pp 527−557, Kluwer Academic Publishers, Dordrecht, The Netherlands.
8. Aumeier, W., Eberl, U., Ogrodnik, A., Volk, M., Scheidel, G., Feick, R., Plato, M., and Michel-Beyerle, M.-E. (1990) in *Current Research in Photosynthesis* (Baltscheffsky, M., Ed.) Vol. I, pp 133−136, Kluwer Academic Publishers, Dordrecht, The Netherlands.
9. Kirmaier, C., Holten, D., and Parson, W. W. (1985) *Biochim. Biophys. Acta 810*, 33−48.
10. Bixon, M., Jortner, J., Michel-Beyerle, M.-E., and Ogrodnik, A. (1989) *Biochim. Biophys. Acta 977*, 273−286.
11. Heller, B. A., Holten, D., and Kirmaier, C. (1995) *Science 269*, 940−945.
12. Holten, D., Windsor, M. W., Parson, W. W., and Thornber, J. P. (1978) *Biochim. Biophys. Acta 501*, 112−126.
13. Lin, S., Jackson, J. A., Taguchi, A. K. W., and Woodbury, N. W. (1999) *J. Phys. Chem. B 103*, 4757−4763.
14. Kolbasov, D., and Scherz, A. (2000) *J. Phys. Chem. B 104*, 1802−1809.
15. Kirmaier, C., Weems, D., and Holten, D. (1999) *Biochemistry 38*, 11516−11530.
16. de Boer, A. L., Neerken, S., de Wijn, R., Permentier, H. P., Gast, P., Vijgenboom, E., and Hoff, A. J. (2001) *Photosynth. Res.* (in press).
17. Katilius, E., Turanchik, T., Lin, S., Taguchi, A. K. W., and Woodbury, N. W. (1999) *J. Phys. Chem. B 103*, 7386−7389.
18. Laible, P. D., Kirmaier, C., Holten, D., Tiede, D. M., Schiffer, M., and Hanson, D. K. (1998) in *Photosynthesis: Mechanisms and Effects* (Garab, G., Ed.) Vol. II, pp 849−852, Kluwer Academic Publishers, Dordrecht, The Netherlands.
19. Ridge, J. P., van Brederode, M. E., Goodwin, M. G., van Grondelle, R., and Jones, M. R. (1999) *Photosynth. Res. 59*, 9−26.
20. McAuley, K. E., Fyfe, P. K., Ridge, J. P., Isaacs, N. W., Cogdell, R. J., and Jones, M. R. (1999) *Proc. Natl. Acad. Sci. U.S.A. 96*, 14706−14711.
21. Paddock, M. L., Rongey, S. H., Feher, G., and Okamura, M. Y. (1989) *Proc. Natl. Acad. Sci. U.S.A. 86*, 6602−6606.
22. Otte, S. C. M. (1992) Dissertation, Leiden University, Leiden, The Netherlands.
23. Visser, J. W. M. (1975) Dissertation, Leiden University, Leiden, The Netherlands.
24. Shochat, S., Gast, P., Hoff, A. J., Boender, G. J., van Leeuwen, S., van Liemt, W. B. S., Vijgenboom, E., Raap, J., Lugtenburg, J., and de Groot, H. J. M. (1995) *Spectrochim. Acta A 51*, 135−144.
25. Kennis, J. T. M., Streltsov, A. M., Aartsma, T. J., Nozawa, T., and Amesz, J. (1996) *J. Phys. Chem. 100*, 2438−2442.
26. Kennis, J. T. M., Streltsov, A. M., Permentier, H., Aartsma, T. J., and Amesz, J. (1997) *J. Phys. Chem. B 101*, 8369−8374.
27. Franken, E. M., Shkuropatov, A. Y., Francke, C., Neerken, S., Gast, P., Shuvalov, V. A., Hoff, A. J., and Aartsma, T. J. (1997) *Biochim. Biophys. Acta 1319*, 242−250.
28. Kirmaier, C., He, H., and Holten, D. (2001) *Biochemistry 40*, 12132−12139.
29. McAuley, K. E., Fyfe, P. K., Ridge, J. P., Cogdell, R. J., Isaacs, N. W., and Jones, M. R. (2000) *Biochemistry 39*, 15032−15043.
30. Stilz, H. U., Finkele, U., Holzapfel, W., Lauterwasser, C., Zinth, W., and Oesterhelt, D. (1994) *Eur. J. Biochem. 223*, 233−242.
31. Stowell, M. H., McPhillips, T. M., Rees, D. C., Soltis, S. M., Abresch, E., and Feher, G. (1997) *Science 276*, 812−816.
32. Arlt, T., Dohse, B., Schmidt, S., Wachtveitl, J., Laussermair, E., Zinth, W., and Oesterhelt, D. (1996) *Biochemistry 35*, 9235−9244.
33. Ermler, U., Fritzsch, G., Buchanan, S. K., and Michel, H. (1994) *Structure 2*, 925−936.
34. Kraulis, P. J. (1991) *Appl. Crystallogr. 24*, 946−950.

BI011450M